Journal of Experimental Botany, Vol. 64, No. 2, pp. 507–517, 2013
doi:10.1093/jxb/ers344 Advance Access publication 1 December, 2012
This paper is available online free of all access charges (see http://jxb.oxfordjournals.org/open_access.html for further details)

Journal of Experimental Botany
www.jxb.oxfordjournals.org

RESEARCH PAPER

Characterization of rapid intervascular transport of cadmium in rice stem by radioisotope imaging

Natsuko I. Kobayashi, Keitaro Tanoi*, Atsushi Hirose and Tomoko M. Nakanishi

Graduate School of Agricultural and Life Sciences, The University of Tokyo, 1–1-1 Yayoi, Bunkyo-ku, Tokyo 113–8657, Japan

* To whom correspondence should be addressed. E-mail: uktanoi@mail.ecc.u-tokyo.ac.jp

Received 27 May 2012; Revised 31 October 2012; Accepted 1 November 2012

Abstract

Participation of the intervascular transport system within the rice stem during cadmium (Cd) partitioning was investigated by characterizing ^{109}Cd behaviour in the shoot. In addition, ^{45}Ca, ^{32}P, and ^{35}S partitioning patterns were analysed for comparison with that of ^{109}Cd. Each tracer was applied to the seedling roots for 15 min, and the shoots were harvested either at 15 min (i.e. immediately after tracer application) or at 48 h. Distribution patterns of each element at 15 min were studied to identify the primary transport pathway before remobilization was initiated. ^{32}P was preferentially transported to completely expanded leaf blades having the highest transpiration rate. The newest leaf received minimal amounts of ^{32}P. In contrast, the amount of ^{35}S transported to the newest leaf was similar to that transported to the other mature leaf blades. Preferential movement towards the newest leaf was evident for ^{109}Cd and ^{45}Ca. These results directly indicate that elemental transport is differentially regulated in the vegetative stem as early as 15 min before the elements are transported to leaves. Cd behaviour in the stem was investigated in detail by obtaining serial section images from the bottom part of shoots after ^{109}Cd was applied to a single crown root. At 30 min, the maximum amount of ^{109}Cd was distributed in the peripheral cylinder of the longitudinal vascular bundles (PV) and, interestingly, some amount of ^{109}Cd was transported downwards along the PV. This transport manner of ^{109}Cd provides evidence that Cd can be loaded on the phloem at the stem immediately after Cd is transported from the root.

Key words: Autoradiography, cadmium, calcium, phosphate, radioisotope, rice, sulphate, tracer, transport, xylem-to-phloem.

Introduction

Minerals taken up by the plant roots are transported to the shoot and distributed to each leaf and the meristem to maintain proper growth. Primary long-distance transport from the roots to the shoot is assumed to be driven by transpiration flow and root pressure within xylem vessels (Marschner, 1995). After translocation to the leaf, minerals are loaded into the phloem and exported from the old tissue to the developing young tissue at a low transpiration rate. This step known as remobilization occurs depending on the kind of solute. In addition to these transport steps, intervascular transport systems in the stem tissue, such as xylem-to-phloem transfer, have been suggested to be of particular importance for elemental partitioning among shoot tissues (Marschner, 1995). The nutrient circulation model coordinating these transport processes within a whole plant has been described particularly for N and K^+/Na^+ based on an analysis of the xylem sap and phloem exudate (Wolf *et al.*, 1991; Pate and Jeschke, 1995; Jeschke and Hartung, 2000).

Cadmium (Cd) is a toxic metal that causes serious problems for plants and animals, including humans (Yanagisawa *et al.*, 1984). Decreasing Cd accumulation in edible parts is important to reduce Cd intake. Cd moves in both the xylem and phloem (Reid *et al.*, 2003; Riesen and Feller, 2005; Hart *et al.*, 2006; Tanaka *et al.*, 2007; Lu *et al.*, 2008; Mori *et al.*, 2009; Uraguchi *et al.*, 2009). In rice, Cd transport from the root to the shoot is xylem dependent (Uraguchi *et al.*, 2009),

while most Cd in the grain is assumed to have been transported by the phloem (Tanaka *et al.*, 2007). Given that Cd could be transported from the roots to the grain through the vascular system in the stem without going through mature leaves (Kashiwagi *et al.*, 2009; Fujimaki *et al.*, 2010; Rodda *et al.*, 2011), it could be supposed that Cd transfer from the xylem to the phloem in the stem could play a role in Cd accumulation in the grain. Transfer cells present in the nodes (Zee, 1972; Kawahara *et al.*, 1975) may play a role in Cd loading of the phloem (Fujimaki *et al.*, 2010). However, the significance of the stem vascular systems for Cd partitioning has not been fully clarified. Indeed, little evidence is available about the actual Cd transport pathway within the stem.

Many recent studies describing the elemental transport mechanism have focused on characterizing ion transporters using ion specificity, transport kinetics, and elemental accumulation patterns. The Cd-efflux transporter OsLCT1 has been suggested to participate in Cd remobilization in the leaf and during intervascular transfer of Cd in rice (Uraguchi *et al.*, 2011). This is based on the result that *OsLCT1* expression levels are high in the flag leaf blade and the uppermost node of the culm and that the Cd content in the grains and phloem exudate from the leaf is reduced in RNAi plants (Uraguchi *et al.*, 2011). The potential importance of the uppermost node in the culm for the intervascular Cd transfer has also been suggested by the Cd accumulation pattern in this tissue (Yamaoka *et al.*, 2010; Yamaguchi *et al.*, 2012). Similarly, molecular biological evidence demonstrating the significance of the stem for boron partitioning in *Arabidopsis*, and silicon and iron partitioning in rice has been reported (Tanaka *et al.*, 2008; Yamaji and Ma, 2009; Kakei *et al.*, 2012). Based on previous studies, consideration has been given to the intervascular transport systems within the stem during the primary ion transport process before they reach leaves.

The elemental transport pathway must be identified to understand the mechanisms determining ion partitioning within the stem. Subsequently, the elemental transport pathway should be described by tracking actual elemental movement as direct evidence instead of using the accumulation pattern or the solute composition in the xylem and phloem. Applying radioisotope-labelled-tracer experiments is an effective approach for this purpose particularly because it enables the discrimination between elements that are already present in the plant and those that are newly absorbed by the roots. Furthermore, remobilization flow and primary elemental transport must be distinguished to specify the characteristics of the intervascular transport systems within the stem. Thus, in this study, tissue partitioning of a labelled tracer was determined 15–30 min after absorption from the roots and before contribution of the remobilization flow on the tracer partitioning pattern increased. The partitioning patterns of ^{32}P, ^{35}S, ^{45}Ca, and ^{109}Cd were determined to identify the features of the Cd vascular transport system. Then, the preferential transport towards the developing sink leaf and the immediate transport directed downwards were demonstrated as a feature of Cd transport, suggesting that phloem transport of Cd occurred during the primary transport process in the vegetative rice stem.

Materials and methods

Plant materials and growth conditions

Seeds of rice (*Oryza sativa* L. 'Nipponbare') were washed with deionized water, submerged for 18 h, and transferred to 0.5 mM $CaCl_2$ solution. After 2 days, seedlings were transferred to half-strength Kimura B nutrient solution (pH 5.6) Tanoi *et al.*, 2011 and grown in a growth chamber under a 16/8 light/dark cycle at 28 °C with 70% humidity. Seedlings with an expanding fifth leaf were pre-cultured in a nutrient solution containing 0.1 μM $CdCl_2$ for 2 days. Next, seedlings in which the seventh leaf was emerging were treated with a radioactive tracer as described below.

Seedlings with an emerging eighth leaf were transferred to a greenhouse under a light/dark cycle at 30/25 °C with natural light and grown in half-strength Kimura B nutrient solution (pH 5.6) for 40 days for sequential section analysis. Mature plants were used for analysis 1 week after addition of 0.1 μM $CdCl_2$ to the nutrient solution.

Measurement of the transpiration rate

The intact leaf transpiration rate in seedlings in which the seventh leaf was emerging was measured in the growth chamber during the light period. For measurement, a portable photosynthesis system (LI-6400, LI-COR, Nebraska) with an attached leaf chamber whose top side was covered with a transparency film to enable the transpiration measurement under the same light condition as the growth chamber (6400–11, LI-COR) was used. The concentration of carbon dioxide in the air in the leaf chamber was fixed at 0.4%. The sample size of the leaves was four for each L4, L5, and L6 blade.

Plant tracer treatment

The roots of young seedlings on which the sixth leaf was emerging were treated for 15 min with 0.05 × Kimura B nutrient solution containing 0.01 μM $CdCl_2$ and radioisotope tracer in a bright growth chamber at 30 °C. A carrier-free solution of $H_3{}^{32}PO_4$ (100 MBq l^{-1}), $H_2{}^{35}SO_4$ (300 MBq l^{-1}), $^{45}CaCl_2$ (500 MBq l^{-1}), or $^{109}CdCl_2$ (200 MBq l^{-1}) was added to the nutrient solution. To analyse the first stages of transport, the aerial parts of three seedlings were harvested immediately at the end of tracer treatment (15 min). The labelled seedlings were transplanted into half-strength Kimura B nutrient solution (pH 5.6) containing 0.1 μM $CdCl_2$ and further incubated for 48 h for translocation analysis. Seedlings were also harvested at 1 and 3 h after initiation of treatment for ^{109}Cd analysis. Each experiment was performed at least twice.

A mature plant at the end of the vegetative stage was used for sequential section analysis. A single crown root emerging from the middle of the stem was treated for 30 min with a ^{109}Cd-containing solution (prepared as described above) by placing the root and solution into a straw-shaped plastic bag in a bright growth chamber. After treatment, the bottom 2 cm of the aboveground shoot part and the labelled crown root on the surface were sampled and sectioned as described below.

Analysis of tracer distribution by autoradiography

The aerial parts of the seedlings treated with the tracers were separated into leaf blades, leaf sheaths, and bottom parts of the shoot including the stem. The leaves were named L2–L8, in order of development from the oldest to the youngest leaf. Although rice plants have two other small leaves, the coleoptile and the first incomplete leaf (L1), these were excluded from analysis. L8 was only visible in seedlings sampled at 48 h. L2 and L7 were not separated into sheaths and blades. The entire L2 leaf was designated as the L2 sheath. L7, which was just emerging from the top of the L6 sheath at the time of sampling, was designated the L7 blade because the sheath was too short to be harvested separately. The partitioning of tracers between individual leaf parts, excluding the coleoptile and L1, were placed in contact with the imaging plates (BAS IP MS, GE Healthcare UK, Buckinghamshire, UK) at 4 °C. The image on the imaging plate was scanned with an FLA5000 image analyser (Fujifilm, Tokyo, Japan) at a resolution of 100 μm. The net photostimulated luminescence intensities in each leaf part were calculated

using image analysis software (Image Gauge version 4.0, Fujifilm). The amount of tracer contained in each leaf part was reported relative to the photostimulated luminescence intensity in the L3 sheath.

Measurement of ^{109}Cd radioactivity

The leaves of seedlings labelled with ^{109}Cd for 15 min were air dried and shredded. Samples were then placed in test tubes, and ^{109}Cd activity in each leaf was quantified using a well-type NaI(Tl) scintillation counter (ARC-300, Aloka, Tokyo, Japan). The counts per minute per leaf were calculated. Blades and sheaths were combined for this measurement.

Preparation of serial sections and autoradiography

Seedlings and a mature plant were labelled as described above before preparation of the serial sections. After the aerial part was harvested and the root was cut off, the bottom part of the aboveground shoot was immediately frozen by submerging in liquid nitrogen. Sliced sections were prepared according to a previously described method (Kawamoto, 2003). Each shoot sample was embedded in embedding medium, covered with adhesive film (Cryo-Film transfer kit, Finetec, Tokyo, Japan), and sliced with a cryostat into serial sections of 30-µm thickness. A BAS IP TR imaging plate (GE Healthcare) was stuck to the frozen section on the side directly opposite the attached film. The imaging plate (IP) with the samples was kept in the freezer at −80 °C for either 5 days (for samples from young seedlings) or 2 weeks (for samples from mature plants). IP was scanned with an FLA5000 image analyser at a resolution of 10 µm to obtain an image of the tracer distribution pattern. The sectioning experiments were performed either in two replications for seedlings or once for mature plants.

Results

Transpiration rate of each leaf

The transpiration rates in L5 and L6 were higher than that in L4 (Table 1). At this growth stage, the tip of the L7 blade was just emerging from the L6 sheath in the shape of a scroll. Therefore, the transpiration rate in the L7 blade could not be analysed although it had been developed almost completely in size.

Distribution patterns of ^{32}P, ^{35}S, and ^{45}Ca in the leaf sheaths and blades after 15 min and 48 h

Fifteen minutes after the initiation of incubation, the amount of ^{32}P found in the L4, L5, and L6 blades was higher than that transported to other parts (Fig. 1A). Among these three blades, the L6 blade showed the highest accumulation of ^{32}P (Fig. 1A). The amount of ^{32}P distributed in the L7 blade within 15 min was less than one-third of that distributed in the L5 blade (Fig. 1A). At 48 h, the amount of ^{32}P transferred to the shoot was 10,000-times higher than that transferred at 15 min (Fig. 1A, B). The ratio of the L7 to L3 sheaths particularly increased to approximately the same as that of the L6 blade (Fig. 1B). The distribution pattern of ^{32}P among the other leaves at 48 h was similar to that at 15 min (Fig. 1A, B). The blade/sheath ratio of ^{32}P amount varied from 1.2 to approximately 4 (Fig. 1A, B).

Fifteen minutes after the initiation of incubation, the amount of ^{35}S transported to the L7 blade was the same as that transported to the L4 and L5 blades. The amount of ^{35}S transported to L6 was 18% higher than that transported to L4, L5, and L7. After 48 h, the maximum amount of ^{35}S was observed in L7, which contained almost twice the amount detected in the L5 and L6 blades (Fig 1D). The total amount of ^{35}S transported to the shoot at 48 h was approximately 50-times higher than that transported at 15 min (Fig. 1C, D).

The distribution pattern of ^{45}Ca 15 min after the initiation of treatment was very different from that of ^{32}P and ^{35}S. Nearly all ^{45}Ca was found in L7 (Fig. 1E). No ^{45}Ca was detected in the L3, L4, L5, or L6 blades (Fig. 1E). However, the distribution pattern of ^{45}Ca was more similar to that of ^{32}P and ^{35}S after 48 h (Fig. 1B, D, F). The amount of ^{45}Ca distributed in the L3–L6 blades was twice as high as that distributed in the sheaths (Fig. 1F). L7 contained approximately the same amount of ^{45}Ca as the L4, L5, and L6 blades (Fig. 1F). The total amount of ^{45}Ca transported to the shoot at 48 h was approximately 11,000-times higher than that transported at 15 min (Fig. 1E, F).

At the end of 15 min, the distribution patterns of ^{45}Ca in the L7 and L3–L6 sheaths were completely different (Fig. 1G). In the case of L7, ^{45}Ca was distributed throughout the leaf (Fig. 1G). In contrast, the amount of ^{45}Ca in the sheaths was very low and mainly distributed at the bottom parts of the sheaths, gradually lessening in intensity towards the tip (Fig. 1G). The distribution pattern of ^{45}Ca observed at 15 min was not observed after 48 h, as ^{45}Ca was distributed uniformly throughout the organs (Fig. 1H).

Table 1. Transpiration rate of L4, L5, and L6 blades in rice seedling L6 is the youngest expanded leaf. Data are means ± SD of measurements from four leaves.

Blade	Transpiration rate (mmol H_2O m^{-2} s^{-1})
L6	3.19 ± 0.718
L5	2.99 ± 0.859
L4	1.90 ± 0.237

Distribution of ^{109}Cd in the leaf sheath and blade over time

No visible images in ^{109}Cd distribution could be obtained from IP plates 15 min after the initiation of treatment: therefore, ^{109}Cd was measured using a scintillation counter. The maximum amount of ^{109}Cd was detected in L3 and L4 at 15 min (Fig. 2A). L7 contained very low amount of ^{109}Cd, approximately one-eighth of that in L3 (Fig. 2A). IP could capture ^{109}Cd distribution images 1 h after the initiation of treatment when ^{109}Cd in L7 was particularly high, although the distribution pattern in other leaves was similar to that observed at 15 min (Fig. 2A, B). The distribution pattern at 1 h was confirmed by scintillation counting (data not shown). The amount of ^{109}Cd in the L5 and L6 sheaths within 3 h had increased to approximately the same amount as that transported to the L3 sheath (Fig. 2C). The total amount of ^{109}Cd distributed in the shoot at 3 h was 55-times higher than that distributed at 1 h. After 48 h, the total amount of ^{109}Cd distributed in the shoot increased to 820-times the amount

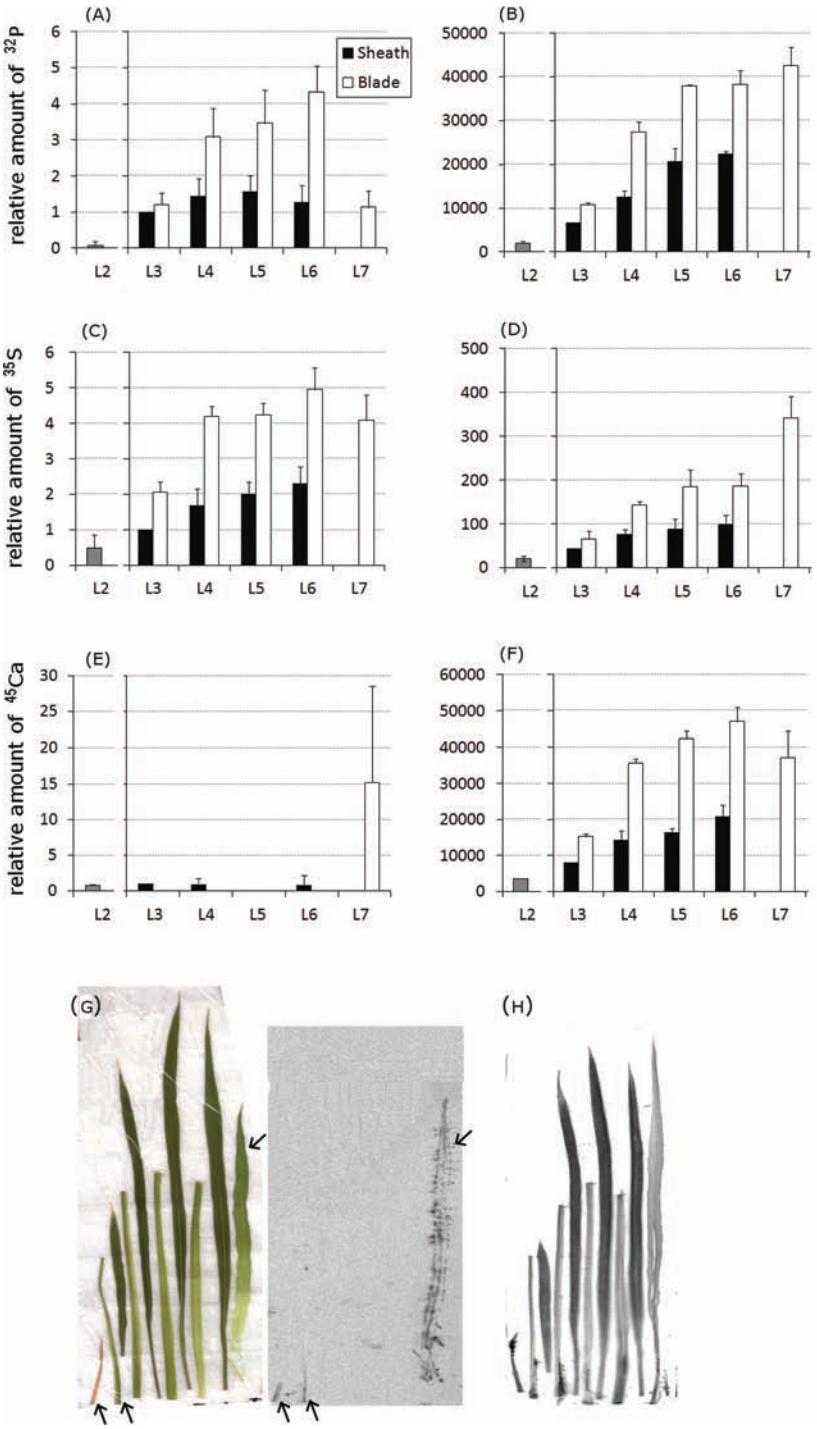

Fig. 1. Distribution patterns of ^{32}P, ^{35}S, and ^{45}Ca in each organ 15 min and 48 h after the initiation of treatment. (A–F) ^{32}P (A, B), ^{35}S (C, D), and ^{45}Ca (E, F) signals were analysed with an imaging plate (IP) at 15 min (A, C, E) and 48 h (B, D, F) after the initiation of treatment. The signal intensity for each organ was based on the photostimulated luminescence value, which was normalized to the value for the L3 sheath of each plant, and was quantified considering the amount of each radionuclide in the L3 sheath at 15 min as a standard. Error bars correspond to standard deviation from three biological repeats. (G, H) Distribution pattern of ^{45}Ca in each organ at 15 min (G) and 48 h (H) are shown in representative IP images. The leaf samples in (G) are shown in order from L2 (far left) to L7 (far right). L3, L4, L5, and L6 were separated into the corresponding sheath and blade (left and right, respectively, in each pair of organs). The photograph of the analysed plant tissues (G, left) shows the positions of the samples in the detected ^{45}Ca image (G, right). Arrows are appended to assist the recognition of ^{45}Ca signals. The leaf samples in (H) were positioned as in (G), except that an L8 image could be detected and is shown at the far right. Experiments were performed at least twice, providing similar results (this figure is available in colour at *JXB* online).

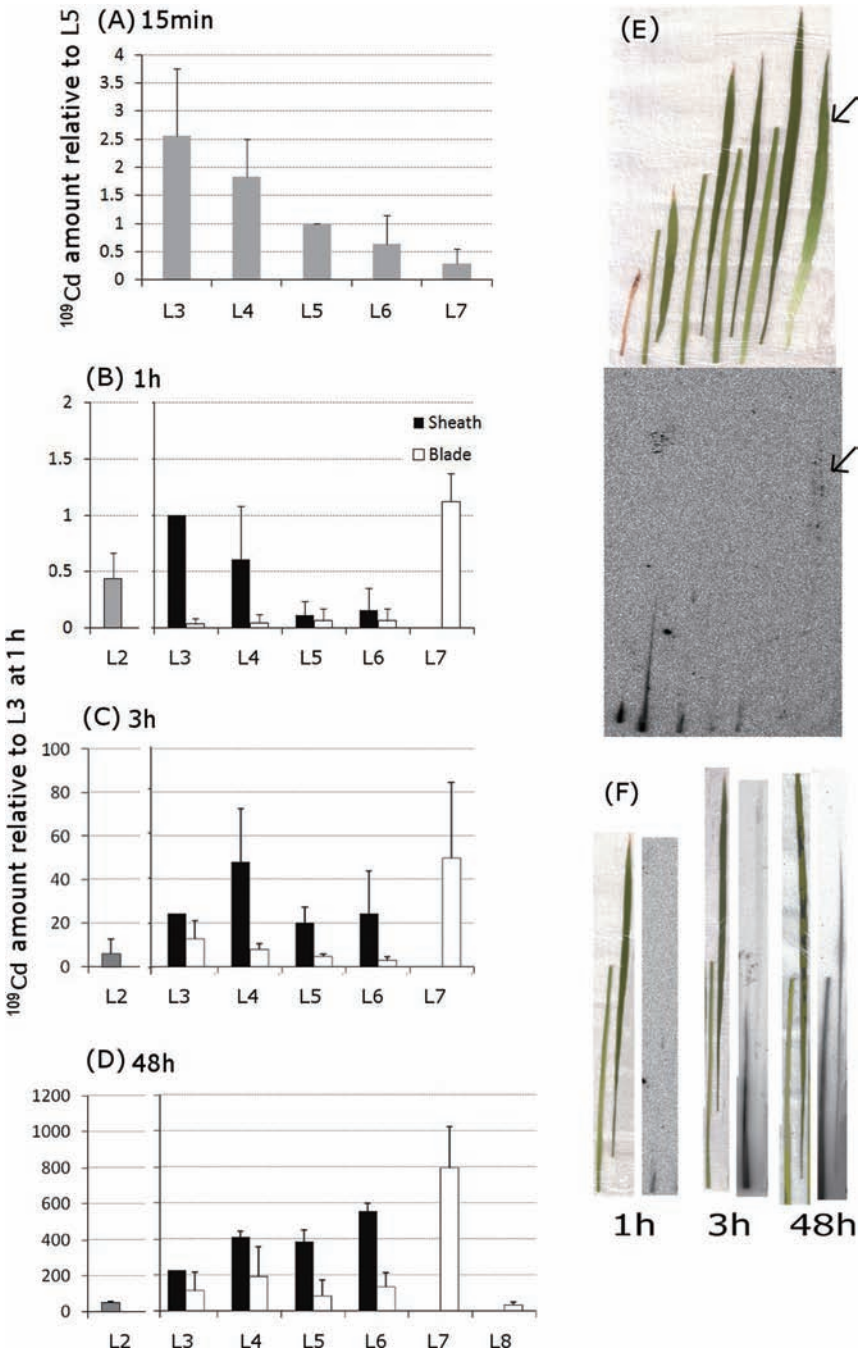

Fig. 2. Time-dependent changes in the distribution pattern of ^{109}Cd in each organ. (A) The amount of ^{109}Cd in the leaves at 15 min was measured using a gamma counter and normalized to that of L5. (B–D) ^{109}Cd signals in the sheath and blade of each leaf were analysed at 1 (B), 3 (C), and 48 h (D) after the initiation of treatment. Signal intensities, based on the photostimulated luminescence values for each organ, were normalized to those of the L3 sheath within each plant. Amount of ^{109}Cd relative to that in the L3 sheath at 1 h was presented. Error bars correspond to standard deviation from three biological repeats. Experiments were performed at least twice, providing similar results. (E) Typical distribution pattern of ^{109}Cd detected by an imaging plate at 1 h (bottom panel) is shown together with a photograph of the organs analysed (top panel). Samples were positioned in order from L2 (far left) to L7 (far right). L3, L4, L5, and L6 were separated into sheaths (left) and blades (right). Arrows are appended to assist the recognition of ^{109}Cd signals in L7. (F) Images of the distribution pattern of ^{109}Cd in L4 at 1, 3, and 48 h after the initiation of treatment. For each time point in (F), the photograph on the left corresponds to the image on the right. Within each panel, the organs are arranged with the sheaths on the left and the blades on the right. Experiments were performed at least twice, providing similar results (this figure is available in colour at *JXB* online).

distributed at 1 h (Fig. 2D). The maximum amount of ^{109}Cd was distributed in L7, which was more than 3-times the amount distributed in the L3 sheath (Fig. 2D). The amount of ^{109}Cd in the L4, L5, and L6 sheaths at 48 h was higher than in the L3 sheath. At 48 h, ^{109}Cd had accumulated at higher amounts in the L3–L6 sheaths than in the blades, which was

different from the distribution patterns of ^{32}P, ^{35}S, and ^{45}Ca (Fig. 1B, D, F and Fig. 2D).

One hour after the initiation of treatment, ^{109}Cd was concentrated in the bottom part of L2, L3, and L4 sheaths, whereas ^{109}Cd signals in L7 were spread throughout the leaf (Fig. 2E). The distribution patterns of ^{109}Cd in the L4 sheath at 1, 3, and 48 h are shown in Fig. 2F. The amount of ^{109}Cd in the L4 organs increased over time, beginning at the bottom of the sheath and gradually spreading upwards (Fig. 2F). ^{109}Cd signals were also found in the L4 blade after 48 h (Fig. 2F).

Distribution of ^{35}S, ^{45}Ca, and ^{109}Cd in sections from the base of the plant at 15 min

The outermost leaves were L3 and L4 in the images of sections taken from the very bottom of the aboveground part of the plant. The stem was located at the centre of each section, which is the base part of L6 and L7, surrounded by L5 (Fig. 3). ^{35}S signals were detected in all leaves and the stem at 15 min, with the maximum radioactivity being detected in the L3 and L4 stem area and vascular tissues (Fig. 3A). The different distribution pattern of ^{35}S among organs, which was accumulated in the vascular tissues in L3 and L4, but not in L5 and the stem, was notable (Fig. 3A). ^{45}Ca signals were detected only in the stem and were absent in L3 and L4 (Fig. 3B). Intense ^{109}Cd signals were detected in vascular tissues of L3, L4, and the stem but not in L5 (Fig. 3C). Unlike ^{35}S, no ^{109}Cd signals were found in the L3 and L4 mesophyll tissues (Fig. 3A, C).

Despite the high amount of ^{109}Cd distributed to the base of L6 and L7 (Fig. 3C), the amount of ^{109}Cd transported to L7 was very low at 15 min, as measured by the gamma counter (Fig. 2A). This contradiction could be accounted for in terms of sample preparation. Indeed, the L7 sample analysed by the gamma counter was cut away from the bottom part of the shoot and did not contain any stem tissue in which ^{109}Cd could accumulate at 15 min. Hence, 15 min was so short that a large amount of ^{109}Cd in the bottom part of the shoot could not enter the L7 blade although it was on track to reach L7.

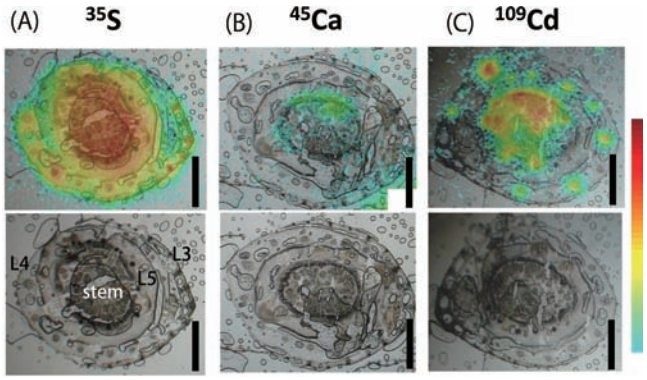

Fig. 3. Distribution patterns of ^{35}S (A), ^{45}Ca (B), and ^{109}Cd (C) in tissues of the bottom part of the shoot 15 min after the initiation of treatment. Signals from tracers detected by the imaging plate are illustrated by a heat map superimposed on the corresponding bright-field image of the section (top row). The bottom row shows the original bright-field images. Bars, 1 mm.

^{109}Cd distribution in sequential sections of the mature plant shoot

A series of sections corresponding to the positions illustrated in Fig. 4 are shown in Fig. 5, from the lowest to the uppermost section. ^{109}Cd was detected in and around the treated crown root, with the maximum amount in the centre (Fig. 5A). ^{109}Cd signals were also detected in one vascular bundle inside the stem and nodal vascular anastomoses (NV) at the centre of the stem (Fig. 5A). NV are connected to the large vascular bundles (LB) and the vertically running small vascular bundles (VSB), and NV ascend upwards around the central cavity (Fig. 4). Both LB and VSB are linked to the PV via the laterally running small vascular bundles (Fig. 4). In the second section (Fig. 5B), the ^{109}Cd-treated crown root is visible beneath the surface of the shoot tissue. ^{109}Cd signals were detected around the treated crown root and in tissues inside the stem, similar to those seen in Fig. 5A (Fig. 5A, B). The ^{109}Cd-treated crown root was further inwards in the stem

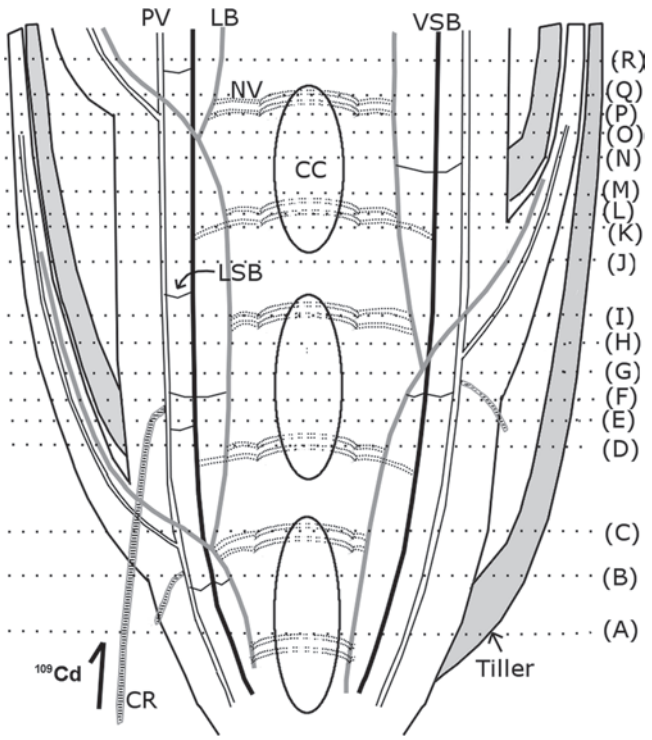

Fig. 4. Schematic illustration of the longitudinal section of a mature rice stem and crown root. ^{109}Cd was supplied to a mature rice plant through one crown root for 30 min (shown at lower left). The shoot was then sliced into sections at the incision lines (A–R) to trace the ^{109}Cd transport pathway inside the stem. The areas between the central cavities are the nodes. CC, central cavity; CR, crown root; LB, large vascular bundles; LSB, laterally running small vascular bundles; NV, nodal vascular anastomoses; PV, peripheral cylinder of longitudinal vascular bundles; VSB, vertically running small vascular bundles.

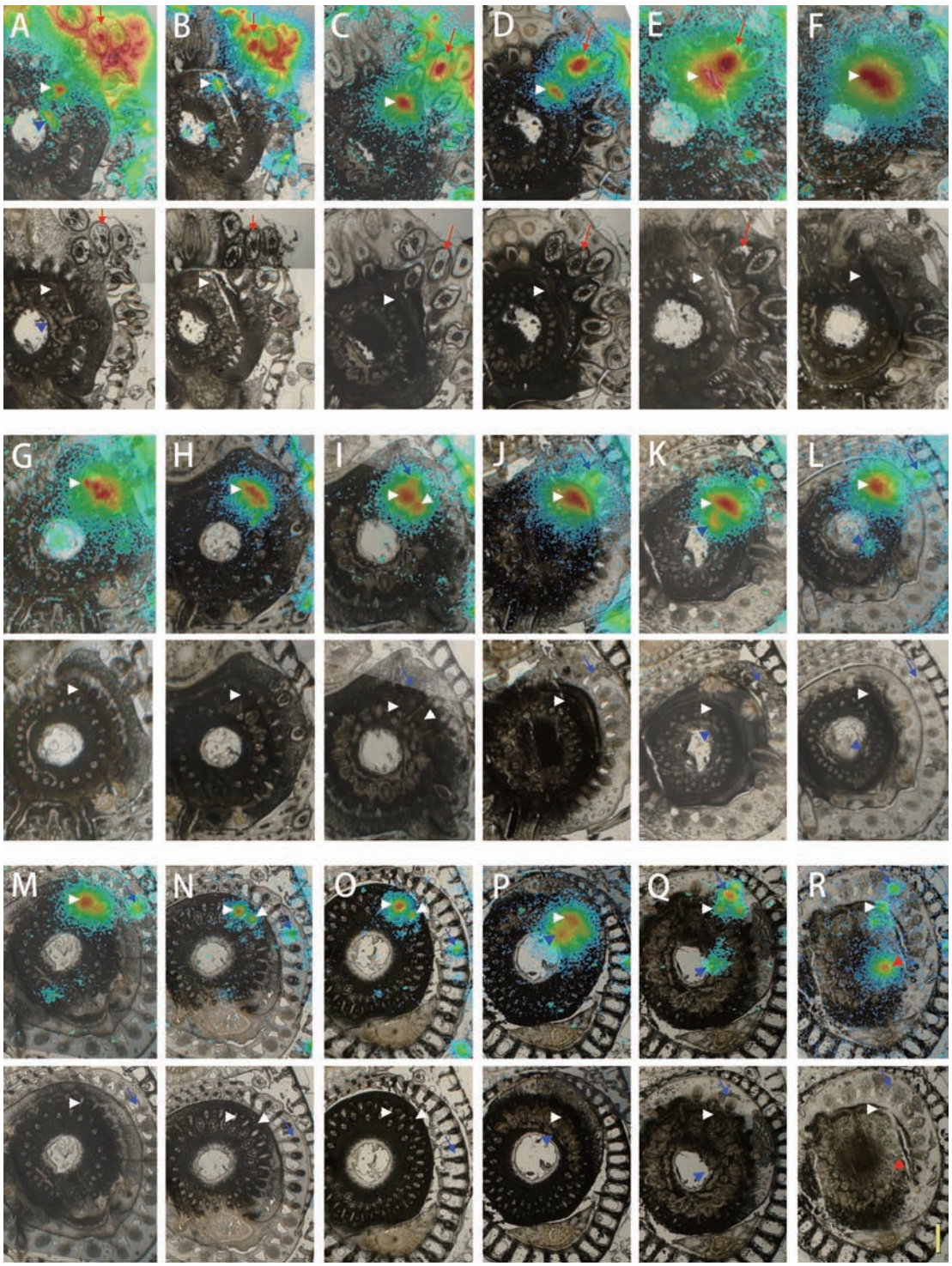

Fig. 5. Serial section images of a mature rice stem after applying ^{109}Cd to one crown root for 30 min. ^{109}Cd signals are illustrated by heat maps superimposed on bright-field images (top panels). The original bright-field images are shown in the bottom panels. The positions of the sections illustrated in (A–R) correspond to the incision lines indicated in Fig. 4. ^{109}Cd signals found in the centre of the treated crown root (red arrows), peripheral cylinder of longitudinal vascular bundles in the stem (white arrowheads), nodal vascular anastomoses (blue arrowheads), the small vascular bundle heading to the leaf (blue arrows), and the large vascular bundle (red arrowheads) are marked as noted. Bar = 1 mm.

in sections from higher positions on the plant (Fig. 5C, D). Intense ^{109}Cd signals were found in the crown root and the tissue around the PV (Fig. 5C, D). In the next section (Fig. 5E), ^{109}Cd was concentrated in the crown root and the PV, which were now located close together inside the stem. In the section shown in Fig. 5F, the shape of the ^{109}Cd-treated crown root can no longer be seen, and intense ^{109}Cd signals were detected along the PV. In the following two sections (Fig. 5G,

5H), ^{109}Cd was maintained in some tissues along the PV. In the next section (Fig. 5I), a small number of ^{109}Cd signals was visible towards the outside of the stem. These signals were located on a small vascular bundle leading into the base of a leaf (Fig. 5I), which was clearly distinguished in the next section (Fig. 5J), where no central cavity was observed at the centre of the stem, indicating the presence of a node. ^{109}Cd was localized mostly in the stem, with some ^{109}Cd detected in the leaf vascular bundle (Fig. 5J). In the next section (Fig. 5K), the leaf base containing a small amount of ^{109}Cd was completely separated from the stem. Some amounts of ^{109}Cd that remained in the stem were also distributed in NV (Fig. 5K). In the next two images (Fig. 5L, M), ^{109}Cd signals were localized in the small leaf vascular bundle and NV around the central cavity. The stem tissue, in which most of ^{109}Cd was localized, was divided into two vascular bundles as shown in Fig. 5M, and even more clearly in the following two sections (Fig. 5N, O). In the next section (Fig. 5P), ^{109}Cd signals were detected within the stem tissue and near the centre of the stem. In the section shown in Fig. 5Q, ^{109}Cd was localized as a small amount in the base of the leaf, the vascular tissues along the PV and NV at the centre of the stem (Fig. 5Q). The last section (Fig. 5R) contained a node (i.e. no central cavity). A new leaf was clearly visible, and the ^{109}Cd signal was detected in a vascular bundle (Fig. 5R). ^{109}Cd was localized within several vascular bundles as well as LB inside the stem (Fig. 5R).

Discussion

In the present study, a ^{109}Cd tracer experiment was performed to detect the primary transport pathway of Cd from the root to the shoot, before secondary translocation began. To achieve early detection of ^{109}Cd signals, a higher level of ^{109}Cd radioactivity (200 MBq l^{-1}) was applied compared with that applied in some previous studies, e.g., 0.6 MBq l^{-1} for 24 h in *Arabidopsis* (Dauthieu *et al.*, 2009), 0.325 MBq l^{-1} for 2 h in soybean (Ohya *et al.*, 2008), and 36 MBq l^{-1} for 4 h in tobacco (Bovet *et al.*, 2006).

According to the transpiration rates in the mature leaves (Table 1) and the observation that L7 was folded in the L6 sheath and was just emerging, L5 and L6 were suggested to be the main target organs for the transpiration stream during this experiment. This suggestion could be supported by the previous observation that completely expanded L5 and L6 leaves have the highest photosynthetic activity and the greatest number of stomata among seedlings with an emerging L7 (Hirasawa *et al.*, 1983). In addition, the consideration that a leaf folded in an older leaf sheath usually has quite a low transpiration rate and is regarded as a sink organ (Matsuo *et al.*, 1995; Tsukamoto *et al.*, 2009) also supports this idea. However, the *in situ* transpiration amount may differ from the transpiration data measured in the measurement device considering the difference in the environment (e.g. the light enters only from the upper side of the device, and the relative humidity in the device was between 45 and 50%).

The ^{32}P distribution pattern at 15 min indicated that phosphorus is initially transported preferentially to tissues with high transpiration rates (Table 1 and Fig. 1A), as was previously reported (Matsuo *et al.*, 1995). The increased proportion of the total amount of ^{32}P found in the L7 blade at 48 h (Fig. 1B) could mostly be a consequence of phosphorus remobilization both in organic and inorganic forms (Hayashi and Chino, 1985).

The ions tested were distributed in a different pattern among the leaves at 15 min during the primary stage of transport (Fig. 1A, C, E and Fig. 3). This variety in distribution pattern cannot be achieved by the transpiration stream alone. Thus, the intervascular transport system in the vegetative stem is clearly involved in the primary elemental transport in an element-specific manner.

The total amount of each tracer in the shoot considerably increased from 15 min to 48 h (Fig. 1A–F). This increase may have been due to the root reserving some of the tracer during the 15-min tracer treatment. The root usually initially reserved an extremely high percentage of the tracer and then gradually released it to the shoot over hours (data not shown).

Considering that L5 and L6 are the target organs for the transpiration stream, the rapid primary transport of ^{45}Ca to the L7 blade at 15 min (Fig. 1E, G and Fig. 2B) demonstrated that ^{45}Ca can be removed from the transpiration stream during passage through the intervascular transport system and redirected rapidly towards the developing young leaf without passing through mature expanded leaves. In contrast, the transpiration flow was assumed to be significant for the Ca distribution pattern in the long term (Fig. 1F, H). Thus, the velocity of Ca transport could be less during transpiration flow than in flow directed to the sink leaf, while a larger amount of Ca was transported by the transpiration stream. The considerable difference between the ^{45}Ca and ^{109}Cd distribution patterns was based on whether they accumulated in the leaf blades or not at 48 h. Once Ca reaches the blade, it is unloaded from the xylem, widely spread throughout the leaf, and gradually accumulated in the blade. In contrast, most Cd is stored in the sheath even at 48 h (Fig. 1F and Fig. 2D). ^{45}Ca was widely spread throughout the leaf, whereas most ^{109}Cd was stored in the sheath, even at 48 h. This characteristic ^{109}Cd distribution pattern of 'sheath > blade' was also found in *Arabidopsis thaliana* in which ^{109}Cd showed the distribution pattern of 'petiole > lamina' within 24 h after ^{109}Cd treatment (Dauthieu *et al.*, 2009). The reason may be that the tissue between the blade and sheath/petiole has ion selectivity that is impervious to Cd and/or that a large difference in complexation ability exists between the sheath/petiole and blade.

Cd is coordinated with O and S in the phloem, whereas most of the Cd is coordinated with S in the xylem (Yamaguchi *et al.*, 2012). Cd binds with low-molecular-weight –SH compounds in the phloem sap (Kato *et al.*, 2010). The different forms of Cd in different tissues may be related to the Cd transport mechanism in the stem. In addition, the mechanisms for lateral elemental transport around vascular tissue, such as the xylem unloading mechanism and subsequent transcellular movement, are different for different elements

(Metzner *et al.*, 2010). In the present study, sulphur was actively unloaded from the xylem, whereas Cd did not leave the vascular tissue of mature leaf sheaths (Fig. 3). Based on the section analysis (Fig. 3C) and quantitative analysis at 15 min (Fig. 2A), it was estimated that the xylem solution supplying in L5 within 15 min contained much less ^{109}Cd than that reaching L3 or L4. Thus, the nodes or internodes allowed Cd to be redirected towards the developing new leaf soon after it reached the stem. In barley seedlings, preferential transport of Fe towards the youngest developing leaf, mostly through the phloem, has been reported as early as 1 h after absorption by the root (Tsukamoto *et al.*, 2009). Recently, the rice iron transporter OsYSL16 has been suggested to be responsible for the phloem loading of iron at the unelongated nodes (Kakei *et al.*, 2012). Although it was not determined whether xylem or phloem is the main route of Cd import in L7 in this study, the Cd-specific intervascular transport system in the stem is suggested to have a considerable effect on Cd partitioning in vegetative Gramineae plants. The possibility that xylem-to-phloem transfer occurred during Cd passage through the vegetative stem was examined by tracing the ^{109}Cd transport pathway in detail. A mature rice plant was used for this examination, because it has a much larger stem than that of a young seedling. However, considering that the mature rice stem has many nodes and internodes stacked within a few centimetres and that the outgrowth of crown roots from the stem internodes is regularly induced, applying ^{109}Cd to the entire root system would allow it to enter the stem tissue from any internode, making it difficult to follow the tracer route. Thus, ^{109}Cd was applied to a single crown root to restrict entrance of the tracer into the stem; this approach resulted in clear images showing the downward Cd transport, which was observed as ^{109}Cd distribution in PV tissue below the connection point of the treated crown root (Fig. 5A–E and Fig. 6). Considering that the PV in which the crown root was formed was connected to the completely expanded upper leaves (Fig. 4), the xylem flow inside was directed upwards. Therefore, downward Cd transport indicated phloem transport of Cd following xylem-to-phloem transfer. Furthermore, the ^{109}Cd distribution pattern around the PV was clearly restricted to a few vascular bundles (Fig. 5C–E) originating from the crown root connection point (Fig. 5F). Based on this ^{109}Cd distribution pattern, it was concluded that ^{109}Cd around the PV was transferred from the xylem to the phloem near the connection point of the crown root (Fig. 6).

Cd transport to the aboveground part is driven by the transpiration stream. The decrease in the Cd transport after abscisic acid treatment is evidence demonstrating this idea (Salt *et al.*, 1995; Zhao *et al.*, 2006; Uraguchi *et al.*, 2009). In the present experiment, ^{109}Cd accumulated in leaves other than the L7 blade at 48 h was shown to be L3 < L4 = L5 < L6 (Fig. 2D), which was consistent with the transpiration amount (Table 1). This ^{109}Cd distribution pattern is consistent with the observation that the main driving force for Cd transport to the shoot is the xylem transpiration stream.

Because the resolution of the images in this study was not sufficiently high to distinguish between the xylem and phloem, it is still unknown whether upward movement of ^{109}Cd in the stem occurs only through the xylem or through both the xylem and phloem. Improvements in imaging techniques will be needed to obtain images with higher resolution to identify the main route for the primary transport of Cd.

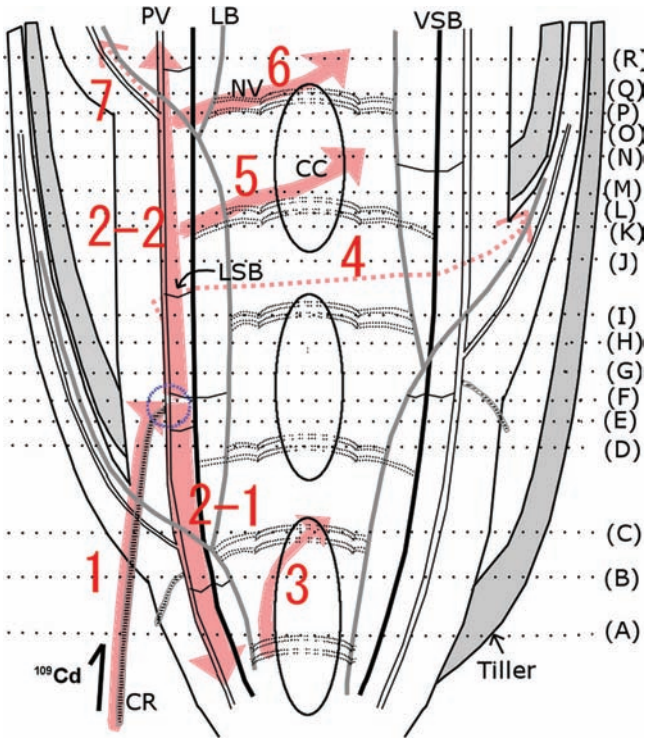

Fig. 6. Schematic presentation of the route of ^{109}Cd in the stem based on an interpretation of the heat maps in Fig. 5. The connection between the crown root (CR) and the main stem is indicated with a blue circle. ^{109}Cd was absorbed by the treated CR (1), then transported both downwards (2–1) and upwards (2–2) inside the stem. Some of the ^{109}Cd that was first transported downwards was further transported to nodal vascular anastomoses (NV) and then upwards along the central cavity (CC) (3). A small amount of ^{109}Cd was transported to the leaves (4, 7), whereas most of the ^{109}Cd remained inside the stem and was distributed both in peripheral cylinder of longitudinal vascular bundles (PV) and NV (5, 6) (this figure is available in colour at *JXB* online).

In conclusion, the autoradiography technique described here, in which only a brief (15-min) pulse treatment of ^{32}P, ^{35}S, ^{45}Ca, or ^{109}Cd was applied to the rice root, provides direct evidence that the intervascular transport system within the vegetative rice stem participates in specific elemental partitioning. The intervascular transport system adjusts the primary transport of Ca and Cd to flow into the sink leaf that was not expanded, whereas the major driving force for these elements from root-to-shoot was transpiration in the mature expanded leaves. The series of frozen section radioisotope images provided evidence that Cd transfer from xylem to phloem can be occurred as soon as Cd was transported from the root to the PV inside the bottom part of the stem. The finding that Cd immediately moves towards the root as well

as towards the sink leaf will be the key to revealing the unique features of the Cd transport pathway inside the stem.

Acknowledgements

This work was supported in part by grants from the Japanese Society for the Promotion of Science to N.I.K. (Research Fellow 22-40171) and to T.M.N. (Funding Program for Next Generation World-Leading Researchers), and from the Ministry of Agriculture, Forestry, and Fisheries of Japan to K.T. (Genomics for Agricultural Innovation grant IPG-0009).

References

Bovet L, Rossi L, Lugon-Moulin N. 2006. Cadmium partitioning and gene expression studies in *Nicotiana tabacum* and *Nicotiana rustica*. *Physiologia Plantarum* **128,** 466–475.

Dauthieu X, Denaix L, Nguyen C, Panfili F, Perrot F, Potin-Gautier M. 2009. Cadmium uptake and distribution in *Arabidopsis thaliana* exposed to low chronic concentrations depends on plant growth. *Plant and Soil* **322,** 239–249.

Fujimaki S, Suzui N, Ishioka NS, Kawachi N, Ito S, Chino M, Nakamura S. 2010. Tracing cadmium from culture to spikelet: noninvasive imaging and quantitative characterization of absorption, transport, and accumulation of cadmium in an intact rice plant. *Plant Physiology* **152,** 1796–1806.

Hart JJ, Welch RM, Norvell WA, Kochian LV. 2006. Characterization of cadmium uptake, translocation and storage in near-isogenic lines of durum wheat that differ in grain cadmium concentration. *New Phytologist* **172,** 261–271.

Hayashi H, Chino M. 1985. Nitrate and other anions in the rice phloem sap. *Plant and Cell Physiology*. **26,** 325–330.

Hirasawa T, Araki T, Matsuda E, Ishihara K. 1983. On exudation rate from the base of the leaf blade in rice plants. *Japanese Journal of Crop Science* **52,** 574–581.

Jeschke WD, Hartung W. 2000. Root-shoot interactions in mineral nutrition. *Plant and Soil* **226,** 57–69.

Kakei Y, Ishimaru Y, Kobayashi T, Yamakawa T, Nakanishi H, Nishizawa NK. 2012. *Os*YSL16 plays a role in the allocation of iron. *Plant Molecular Biology* **79,** 583–594.

Kashiwagi T, Shindoh K, Hirotsu N, Ishimaru K. 2009. Evidence for separate translocation pathways in determining cadmium accumulation in grain and aerial plant parts in rice. *BMC Plant Biology* **9,** 8.

Kato M, Ishikawa S, Igarashi K, Chiba K, Hayashi H, Yanagisawa S, Yoneyama T. 2010. Possible chemical forms of cadmium and varietal differences in cadmium concentrations in the phloem sap of rice plants (*Oryza sativa* L.). *Soil Science and Plant Nutrition* **56,** 839–847.

Kawahara H, Chonan N, Matsuda T. 1975. Studies on morphogenesis in rice plants 8. The morphology of vascular bundles in the dwarf part of stem. *Proceedings of the Crop Science Society of Japan* **44,** 61–67 (in Japanese).

Kawamoto T. 2003. Use of a new adhesive film for the preparation of multi-purpose fresh-frozen sections from hard tissues, whole-animals, insects and plants. *Archives of Histology and Cytology* **66,** 123–143.

Lu LL, Tian SK, Yang XE, Wang XC, Brown P, Li TQ, He ZL. 2008. Enhanced root-to-shoot translocation of cadmium in the hyperaccumulating ecotype of *Sedum alfreddii*. *Journal of Experimental Botany* **59,** 3203–3213.

Marschner H. 1995. *Mineral nutrition of higher plants*, 2nd edn. London, UK: Academic Press.

Matsuo T, Kumazawa K, Ishii R, Ishihara K, Hirata H. 1995. *Science of the rice plant. Volume 2: Physiology*. Tokyo: Nobunkyo.

Metzner R, Thorpe MR, Breuer U, Blumler P, Schurr U, Schneider HU, Schroeder WH. 2010. Contrasting dynamics of water and mineral nutrients in stems shown by stable isotope tracers and cryo-SIMS. *Plant, Cell and Environment* **33,** 1393–1407.

Mori S, Uraguchi S, Ishikawa S, Arao T. 2009. Xylem loading process is a critical factor in determining Cd accumulation in the shoots of *Solanum melongena* and *Solanum torvum*. *Environmental and Experimental Botany* **67,** 127–132.

Ohya T, Iikura H, Tanoi K, Nishiyama H, Nakanishi TM. 2008. Cd-109 uptake and translocation in a soybean plant under different pH conditions. *Journal of Radioanalytical and Nuclear Chemistry* **264,** 303–306.

Pate JS, Jeschke WD. 1995. Role of stems in transport, storage, and circulation of ions and metabolites by the whole plant. In: BL Gardner, editor, *Plant stems, physiology and functional morphology*. San Diego: Academic Press. pp 177–204.

Reid RJ, Dunbar KR, McLaughlin MJ. 2003. Cadmium loading into potato tubers: the roles of the periderm, xylem and phloem. *Plant, Cell and Environment* **26,** 201–206.

Riesen O, Feller U. 2005. Redistribution of nickel, cobalt, manganese, zinc, and cadmium via the phloem in young and maturing wheat. *Journal of Plant Nutrition* **28,** 421–430.

Rodda MS, Li G, Reid RJ. 2011. The timing of grain Cd accumulation in rice plants: the relative importance of remobilisation within the plant and root Cd uptake post-flowering. *Plant and Soil* **347,** 105–114.

Salt DE, Prince RC, Pickering IJ, Raskin I. 1995. Mechanisms of cadmium mobility and accumulation in Indian mustard. *Plant Physiology* **109,** 1427–1433.

Tanaka K, Fujimaki S, Fujiwara T, Yoneyama T, Hayashi H. 2007. Quantitative estimation of the contribution of the phloem in cadmium transport to grains in rice plants (*Oryza sativa* L.). *Soil Science and Plant Nutrition* **53,** 72–77.

Tanaka M, Wallace IS, Takano J, Roberts DM, Fujiwara T. 2008. NIP6;1 is a boric acid channel for preferential transport of boron to growing shoot tissues in *Arabidopsis*. *The Plant Cell* **20,** 2860–2875.

Tanoi K, Saito T, Iwata N, Kobayashi NI, Nakanishi TM. 2011. The analysis of magnesium transport system from external solution to xylem in rice root. *Soil Science and Plant Nutrition* **53,** 265–271.

Tsukamoto T, Nakanishi H, Uchida H, Watanabe S, Matsuhashi S, Mori S, Nishizawa NK. 2009. 52Fe translocation in barley as monitored by a positron-emitting tracer imaging system (PETIS): evidence for the direct translocation of Fe from roots to young leaves via phloem. *Plant and Cell Physiology* **50,** 48–57.

Uraguchi S, Kamiya T, Sakamoto T, Kasai K, Sato Y, Nagamura Y, Yoshida A, Kyozuka J, Ishikawa S, Fujiwara T. 2011. Low-affinity cation transporter (Os*LCT1*) regulates cadmium transport into

rice grains. *Proceedings of the National Academy of Sciences, USA* **108,** 20959–20964.

Uraguchi S, Mori S, Kuramata M, Kawasaki A, Arao T, Ishikawa S. 2009. Root-to-shoot Cd translocation via the xylem is the major process determining shoot and grain cadmium accumulation in rice. *Journal of Experimental Botany* **60,** 2677–2688.

Wolf O, Munns R, Tonnet ML, Jeschke WD. 1991. The role of the stem in the partitioning of Na^+ and K^+ in salt-treated barley. *Journal of Experimental Botany* **42,** 697–704.

Yamaguchi N, Ishikawa S, Abe T, Baba K, Arao T, Terada Y. 2012. Role of the node in controlling traffic of cadmium, zinc, and manganese in rice. *Journal of Experimental Botany*, **63,** 2729–2737.

Yamaji N, Ma JF. 2009. A transporter at the node responsible for intervascular transfer of silicon in rice. *The Plant Cell* **21,** 2878–2883.

Yamaoka W, Takada S, Takehisa H, Hayashi Y, Hokura A, Terada Y, Abe T, Nakai, I. 2010. Study on accumulation mechanism of cadmium in rice (*Oriza sativa* L.) by micro-XRF imaging and X-ray absorption fine structure analysis utilizing synchrotron radiation. *Bunseki Kagaku* **59,** 463–475 (in Japanese).

Yanagisawa M, Niimura Y, Yamada N, Segawa A, Kida K. 1984. Heavy metal pollution and soil replacement in Jinzu River basin. *Bulletin of the Toyama Agricultural Experiment Station* **15,** 1–110 (in Japanese).

Zee SY. 1972. Transfer cells and vascular tissue distribution in the vegetative nodes of rice. *Australian Journal of Botany* **20,** 41–48.

Zhao FJ, Jiang RF, Dunham SJ, McGrath SP. 2006. Cadmium uptake, translocation and tolerance in the hyperaccumulator *Arabidopsis halleri*. *New Phytologist* **172,** 646–654.